

ChemComm

Accepted Manuscript



This is an *Accepted Manuscript*, which has been through the Royal Society of Chemistry peer review process and has been accepted for publication.

Accepted Manuscripts are published online shortly after acceptance, before technical editing, formatting and proof reading. Using this free service, authors can make their results available to the community, in citable form, before we publish the edited article. We will replace this *Accepted Manuscript* with the edited and formatted *Advance Article* as soon as it is available.

You can find more information about *Accepted Manuscripts* in the [Information for Authors](#).

Please note that technical editing may introduce minor changes to the text and/or graphics, which may alter content. The journal's standard [Terms & Conditions](#) and the [Ethical guidelines](#) still apply. In no event shall the Royal Society of Chemistry be held responsible for any errors or omissions in this *Accepted Manuscript* or any consequences arising from the use of any information it contains.

COMMUNICATION

Prato and Bingel-Hirsch cycloaddition to heptagon-containing $\text{LaSc}_2\text{N}@C_5(\text{hept})\text{-C}_{80}$: importance of pentalene units

Cite this: DOI: 10.1039/x0xx00000x

Received 00th January 2012,
Accepted 00th January 2012Qingming Deng^a and Alexey A. Popov^{*a}

DOI: 10.1039/x0xx00000x

www.rsc.org/

Possible cycloaddition sites in the heptagon-containing fullerene $\text{LaSc}_2\text{N}@C_5(\text{hept})\text{-C}_{80}$ are studied computationally. Thermodynamically controlled Prato addition is predicted to proceed regioselectively across the pentagon/pentagon (p/p) edges, whereas in kinetically-controlled Bingel-Hirsch reaction the most reactive are carbons next to the p/p edge.

The prospective applications of endohedral metallofullerenes (EMFs) (such as in photovoltaic or medicine) require derivatization of pristine EMF compounds to improve solubility or introduce functional groups.¹ Therefore, a lot of efforts has been devoted to the understanding of their chemical properties.^{2,3} Both carbon cage topology and the nature of endohedral species can dramatically affect reactivity of EMFs. Furthermore, endohedral metal clusters can stabilize unconventional fullerene cages (such as those containing pentagon pairs), which can lead to unexpected reactivity patterns. Very recently we have discovered the first endohedral metallofullerenes with heptagonal ring, $\text{LaSc}_2\text{N}@C_5(\text{hept})\text{-C}_{80}$ (hereafter the title is shortened to $\text{LaSc}_2\text{N}@C_{80}$ and only $C_5(\text{hept})$ cage is considered unless the otherwise noted).⁴ Its structure has C_5 -symmetric cage with one heptagon fused to two adjacent pentagon pairs (Fig. 1). DFT computations showed that this heptagon-containing EMF has high thermodynamic stability, and it is not unlikely that new EMFs with heptagonal rings may be found in a near future. In this work we analyse how the presence of the heptagon affects the chemical properties of unconventional EMFs. In particular, we perform a systematic computational study of the preferable reaction pathways of Prato and Bingel-Hirsch cycloadditions reactions to heptagon-containing $\text{LaSc}_2\text{N}@C_{80}$ molecule.

In Prato reaction,⁵ amino acid (e.g. sarcosine) reacts with aldehyde to form an ylide, which then reacts with a fullerene CC bond via 1,3-dipolar cycloaddition to form a pyrrolidine ring:

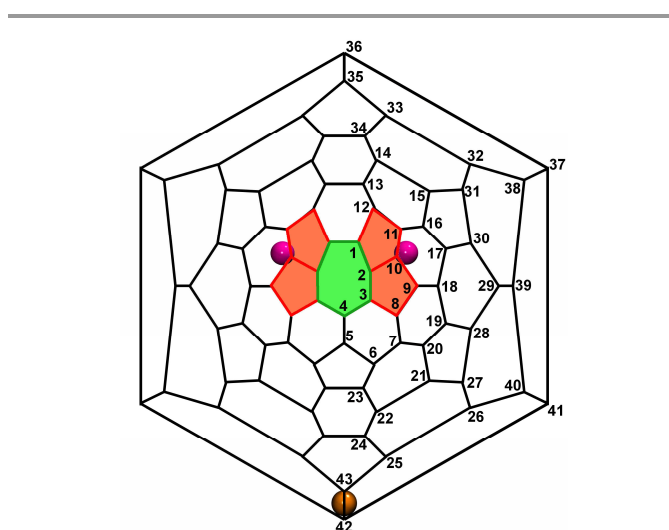
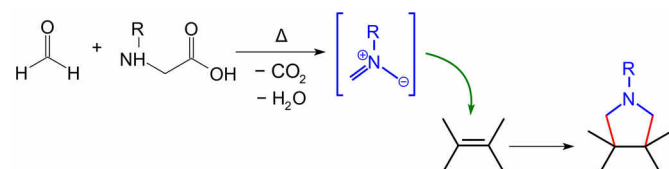


Figure 1. Schlegel diagram of $\text{LaSc}_2\text{N}@C_5(\text{hept})\text{-C}_{80}$ with quasi-spiral numbering system of carbon atoms used in this work. Heptagon and pairs of adjacent pentagons are highlighted in green and red, respectively, whereas position of Sc and La atoms are marked with magenta and orange spheres.



Prato reaction of $\text{M}_3\text{N}@I_h\text{-C}_{80}$ is studied very well both experimentally and computationally.^{2,6,7,8,9} This highly symmetric cage with rotating M_3N cluster has only two addition sites located on pentagon/hexagon and hexagon/hexagon edges (denoted as [5,6] and [6,6], respectively). [5,6] adduct is more preferable for clusters of smaller size (such as Sc_3N), whereas increase of the cluster size stabilizes the [6,6] isomer, which

becomes predominant product for the $\text{Gd}_3\text{N}@C_{80}$.^{6,8} Reaction is known to proceed under thermodynamic control (although kinetic products may be formed first^{8,9}), and hence addition sites can be predicted based on the relative stability of the isomeric adducts.

The C_5 -symmetric cage of $\text{LaSc}_2\text{N}@C_5(\text{hept})-C_{80}$ has 64 inequivalent CC bonds, and all of them can be considered as potential addition sites. Relative energies of the complete list of 64 computed isomers of $\text{LaSc}_2\text{N}@C_{80}(\text{CH}_2)_2\text{NH}$ is given in the Electronic Supporting Information (ESI Table S1). Table 1 lists several most stable isomers and all four heptagon-based adducts. Note that inversion of the pyrrolidine ring and NH fragment yields four conformers for each addition site. For a given addition site the energies of the conformers can vary within 10 kJ/mol. The values discussed hereafter correspond to the lowest energy conformers.

Table 1. Selected $\text{LaSc}_2\text{N}@C_{80}(\text{CH}_2)_2\text{NH}$ isomers, their relative energies and HOMO-LUMO gaps, and corresponding geometry parameters in pristine $\text{LaSc}_2\text{N}@C_{80}$.

CC ^a	Type ^b	ΔE^c	gap _{H-L} ^d	$d(\text{CC})^e$	θ_p^f
2-10	6-[5,5]-7	0.0	1.21	1.445	13.50/15.96
15-31	6-[5,6]-6	31.7	1.11	1.436	10.09/9.97
11-12	6-[5,6]-6	32.4	1.19	1.465	14.27/9.74
20-21	6-[5,6]-6	35.3	1.06	1.436	11.37/10.61
9-10	5-[5,6]-6	36.0	1.16	1.450	13.06/15.96
17-30	5-[5,6]-6	37.0	0.73	1.445	11.21/10.36
13-13'	6-[6,6]-6	38.5	1.33	1.442	7.52/7.52
...					
1-2	5-[5,7]-6	70.9	0.85	1.455	7.33/13.5
2-3	5-[5,7]-6	74.0	0.75	1.465	13.5/7.03
1-1'	5-[6,7]-5	84.8	0.86	1.403	7.33/7.33
3-4	5-[6,7]-6	106.1	0.80	1.461	7.03/7.10

^a addition site, see Fig. 1 for numbering of carbon atoms; ^b numbers in the square brackets denote polygons, whose junction forms addition site, whereas the number before and after square brackets denote the rings at the vertices of the addition site (e.g. 6-[5,6]-7 means pentagon/hexagon edge located between hexagon and heptagon), ^c relative energy, in kJ/mol, ^d HOMO-LUMO gap, in eV; ^e CC bond lengths in pristine $\text{LaSc}_2\text{N}@C_{80}$, in Å; ^f POAV pyramidalization angles, θ_p , of carbon atoms in pristine $\text{LaSc}_2\text{N}@C_{80}$, in °.

Inspection of all optimized $\text{LaSc}_2\text{N}@C_{80}(\text{CH}_2)_2\text{NH}$ isomers showed that one addition site, the **2-10** bond at the pentagon/pentagon junction, is particular preferable for cycloaddition (Fig. 2). Corresponding cycloadduct is separated from all other isomeric adducts by the energy gap of 30 kJ/mol and can be expected to be obtained regioselectively. The HOMO-LUMO gap of the cycloadduct is 1.21 eV, which is slightly higher than the gap in the pristine $\text{LaSc}_2\text{N}@C_{80}$, 1.15 eV. At the same time, both HOMO and LUMO of the adduct (-5.03/-3.81 eV) are destabilized by ca 0.2 eV with respect to the $\text{LaSc}_2\text{N}@C_{80}$ values (-5.23/-4.08 eV).

Among the six addition sites with relative energies between 30 and 40 kJ/mol, five are [5,6] edges, including two [5,6] adducts at the perimeter of the pentalene unit (**11-12**, **9-10**). Remarkably stable is the [6,6] adduct at the **13-13'** bond in the pyrene fragment (carbon atoms at the triple hexagon junctions are usually less reactive).

The lowest energy heptagon-based cycloadduct is the [5,7] adduct across the **1-2** bond (70.9 kJ/mol) followed by another

[5,7] adduct to the **2-3** bond (74.0 kJ/mol). [6,7] adducts are even less stable (84.8 kJ/mol for **1-1'** and 106.1 kJ/mol for **3-4**). In fact, [6,7]-adduct to the **3-4** bond is one of the least thermodynamically stable structures among the whole set of $\text{LaSc}_2\text{N}@C_{80}(\text{CH}_2)_2\text{NH}$ adducts. The highest energy, 128.7 kJ/mol, is found for the adduct across the **7-8** bond.

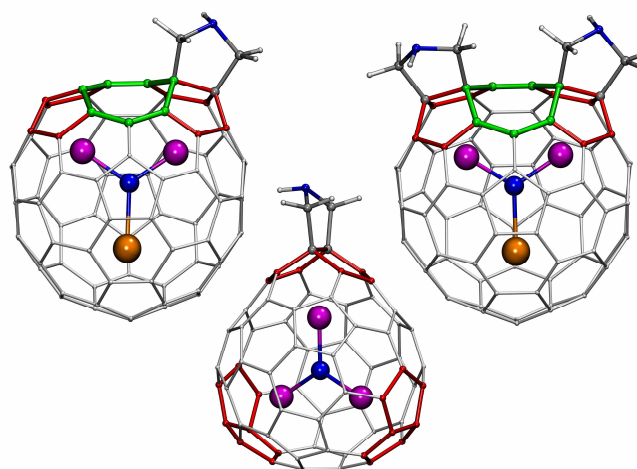


Figure 2. The most stable $\text{LaSc}_2\text{N}@C_{80}(\text{CH}_2)_2\text{NH}$, bis $\text{LaSc}_2\text{N}@C_{80}[(\text{CH}_2)_2\text{NH}]_2$, and $\text{Sc}_3\text{N}@C_{68}(\text{CH}_2)_2\text{NH}$ cycloadducts. Heptagon ring is highlighted in green, pentalene units are highlighted in red. N, Sc and La atoms are blue, magenta and orange, respectively.

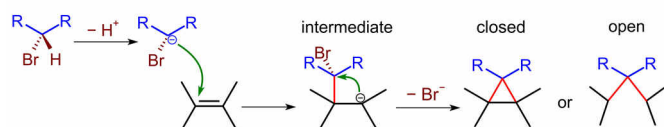
We tried to rationalize relative stability of fulleropyrrolidine cycloadducts based on the CC bond length in the pristine molecule or pyramidalization of carbon atoms (quantified in terms of POAV¹⁰ angles θ_p), but this analysis did not reveal any clear correlation between geometry parameters and preferable reaction sites (Table 1, see also ESI Tables S2 and S3). The atoms C2 and C10 at the [5,5] edge are among the most pyramidal ones in the $\text{LaSc}_2\text{N}@C_{80}$ molecule, so pyramidalization may play a role here. But there is no correlation between pyramidalization angles and relative stabilities for higher energy isomers. For instance, **9-10** adduct in the most pyramidal region of the pristine fullerene (θ_p angles are 13.06/15.96°) has similar stability to the **13-13'** isomer with quite flat carbon atoms ($\theta_p = 7.52^\circ$). Likewise, the bond length also does not correlate with the stability of the adducts. **1-1'** is the shortest CC bond in the pristine fullerene (1.403 Å), but corresponding adducts is rather unstable (84.8 kJ/mol). The **2-10** bond length of the [5,5] edge, 1.445 Å, is in the middle of the CC bond lengths range in the $\text{LaSc}_2\text{N}@C_{80}$, 1.403–1.469 Å. Analysis of the HOMO and LUMO distributions (see ref. 4) also does not give a reasonable guess of the most stable adducts. Thus, it is not possible to rationalize reactivity using simple structural and electronic arguments based on the pristine $\text{LaSc}_2\text{N}@C_{80}$ molecule.

The preference of the cycloaddition across the pentagon/pentagon edge in the pentalene is quite remarkable. To our knowledge, Prato reaction for non-IPR EMFs has not been considered before. Thus, we also computed fulleropyrrolidine adducts of $\text{Sc}_3\text{N}@C_{68}$, whose carbon cage also violates the IPR

and has three pentalene units.¹¹ Computations of the cycloadducts across all 18 non-equivalent CC bonds of the Sc₃N@C₆₈ molecule showed that the most thermodynamically preferable is addition to the [5,5] edge (Fig. 2). Other adducts are higher in energy by at least 20 kJ/mol (see ESI Table S4 for the complete list of isomeric cycloadducts). Thus, enhanced reactivity of the pentagon/pentagon edges in Prato cycloaddition may be a general rule for non-IPR EMFs. Furthermore, this reactivity pattern is likely to be common for some other cycloaddition reactions such as Diels-Alder addition.¹²

The preference for the addition to the [5,5] bond is also preserved if the monoadduct undergoes the second cycloaddition process. Computations of all 118 bis-adducts obtained by (CH₂)₂NH addition to the **2–10** monoadduct of LaSc₂N@C₈₀ showed that the second pentalene unit will be also functionalized with high regioselectivity (see ESI Table S5 for a list of considered bis-adducts) with formation of the C_s-symmetric (**2–10,2'–10'**) bis-adduct (Fig. 2).

In Bingel-Hirsch reaction,¹³ a carbanion formed via proton abstraction from the bromomalonate attacks the fullerene double bond with formation of the intermediate, which then converts to the cycloadduct via removal of the Br[−] anion:



The product can be either “closed” methanofullerene (typical for empty fullerenes¹⁴ and Sc₃N@C₇₈¹⁵) or “open” methanofulleroid (typical for nitride clusterfullerenes^{16,17,18}). Bingel-Hirsch addition to nitride clusterfullerenes is found to be kinetically driven.^{17,18} Alegret *et al.* showed that addition sites can be predicted based on (i) the lowest energy intermediate carbanion, then followed by (ii) the lowest-energy transition state for the Br[−] abstraction.¹⁷

To find the most kinetically-favourable addition sites in LaSc₂N@C₈₀, first we computed all 129 intermediates obtained by addition of CH₂Br anion to symmetry inequivalent cage carbon atoms (for each cage carbon atom, there are three conformers of the [LaSc₂N@C₈₀CH₂Br][−] intermediate with different directions of the C–Br bond, see ESI Table S6). The most stable intermediates are obtained by CH₂Br[−] addition to four carbon atoms around the pentagon/pentagon edge (C1, C3, C9, and C11), and two carbon atoms next to them (C16 and C18) (Table 2). For these intermediates we further computed transition states (TS) for the Br[−] removal. Reaction barriers were found to be in the range of 90–120 kJ/mol (with respect to corresponding intermediates).

Based on the low energy intermediate and reaction barrier, the most kinetically favoured Bingel cycloadduct is **11–16** (Fig. 3). Although the corresponding intermediate is somewhat less stable than the intermediates based on the C1 atom, the barrier to the Br[−] removal in **11–16** is much lower, and hence this cycloadduct is expected to be formed much faster. The HOMO-LUMO gap of **11–16** is 1.15 eV; the energies of the frontier MOs

(−5.01/−3.87 eV) are 0.2 eV higher than in the pristine LaSc₂N@C₈₀.

Table 2. The lowest energy [LaSc₂N@C₈₀CH₂Br][−] intermediates (ΔE_i), transition states of Br[−] removal (ΔE_{TS}), and relative energies of corresponding LaSc₂N@C₈₀CH₂ cycloadducts (ΔE_{CA})^a

CC ^b	ΔE_i	ΔE_{TS}^c	ΔE_{CA}	CC ^b	ΔE_i	ΔE_{TS}^c	ΔE_{CA}
1–12	0.0	115.9	46.8	16–17	13.4	101.1	16.7
1–2	1.6	124.2	34.9	16–15	15.4	117.7	82.3
1–1'	5.2	120.0	102.7	16–11	17.7	97.1	51.8
11–16	7.7	95.1	51.8	9–18	18.1	90.7	7.7
11–12	9.3	100.0	34.0	9–8	19.6	109.7	31.5
11–10	11.9	107.0	8.2	9–10	24.4	93.9	28.9
3–8	12.2	95.7	17.1	18–17	21.9	98.3	7.4
3–4	16.2	109.5	38.0	18–19	22.1	102.3	74.3
3–2	19.1	107.4	5.3	18–9	24.4	96.9	7.7
42–41	29.3	89.3	16.1	42–43	29.9	92.0	0.0

^a all values in kJ/mol; ^b the first number is the carbon atom to which the carbanion is bonded in the intermediate, the second one – the atom which forms new C–C bond in the process of Br[−] abstraction; ^c TS energies are referred to corresponding intermediates.

Taking into account possible uncertainties of few kJ/mol in DFT calculations, the adducts **1–12**, **3–8** (Fig. 3), **9–18** and **11–12** cannot be fully excluded. All kinetically favoured structures have rather high relative energies and thus are not favoured thermodynamically (e.g., relative energy of **11–16** is 51.8 kJ/mol). The most thermodynamically stable LaSc₂N@C₈₀CH₂ isomer is obtained by addition across the **42–43** bond, which is coordinated by the La ion. Because of the relatively unstable intermediate (29.9 kJ/mol), this adduct is not favoured kinetically.

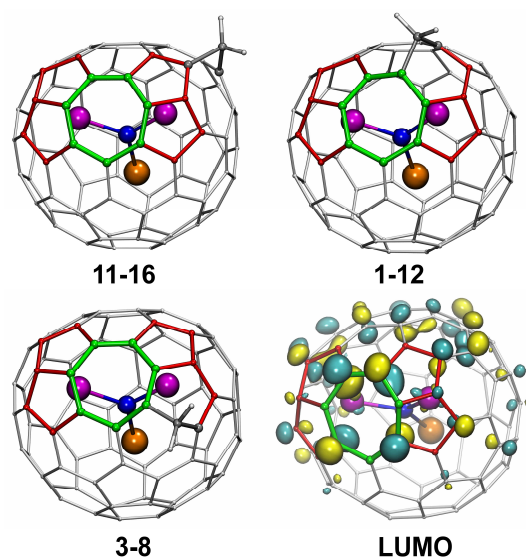


Figure 3. The most kinetically favoured LaSc₂N@C₈₀CH₂ adducts: **11–16**, **1–12**, **3–8**. Also shown is the LUMO of LaSc₂N@C_s(hept)-C₈₀.

Interestingly, the **11–16** site of LaSc₂N@C₈₀ is similar to the most favourable addition site in Bingel-Hirsch cycloaddition to Sc₃N@C₆₈ (see refs. ^{17,18} and ESI Figure S1) and to Gd₃N@C_{82,84}.¹⁹ Thus, similar to Prato reaction, reactivity of non-IPR nitride clusterfullerenes in Bingel-Hirsch reaction is dictated

by the pentalene units, whereas the heptagon edges remain non-functionalized. We could not find unequivocal correlation between the structural parameters of the pristine $\text{LaSc}_2\text{N@C}_{80}$ and the reactivity. At the same time, analysis of the frontier MOs shows that the most stable $[\text{LaSc}_2\text{N@C}_{80}\text{CH}_2\text{Br}]^-$ intermediates are formed with the cage atoms having the highest LUMO coefficients in the pristine $\text{LaSc}_2\text{N@C}_{80}$ molecule (Figure 3). Likewise, Bingel-Hirsch addition to $\text{Sc}_3\text{N@C}_{68}$ proceeds via the carbon atoms with the highest LUMO contribution (see ESI Figure S1).

Conclusions

Detailed computational study of the nitride clusterfullerene $\text{LaSc}_2\text{N@C}_s(\text{hept})\text{-C}_{80}$ showed that C–C bonds at the perimeter of the heptagonal ring are not reactive either in thermodynamically or kinetically controlled cycloaddition reactions. However it would not be correct to claim that the presence of the heptagon has no effect on the chemical reactivity of the molecule. The heptagon induces formation of two pentalene units, and our analysis shows that the most chemically reactive sites in the $\text{LaSc}_2\text{N@C}_s(\text{hept})\text{-C}_{80}$ molecule are related to these structural elements. It is found that thermodynamically controlled Prato reaction should proceed with high regioselectivity across the pentagon/pentagon edges (2–16). In kinetically controlled Bingel-Hirsch cycloaddition, the most reactive site is the CC bond next to the pentalene (11–16). Very similar behaviour is found earlier for other non-IPR nitride clusterfullerene, $\text{Sc}_3\text{N@C}_{68}$, $\text{Gd}_3\text{N@C}_{82}$, and $\text{Gd}_3\text{N@C}_{84}$. Thus, we can conclude that the reactivity pattern described in this work for $\text{LaSc}_2\text{N@C}_s(\text{hept})\text{-C}_{80}$ is common for all non-IPR clusterfullerenes.

Acknowledgements

We thank Ulrike Nitzsche for the help with local computational resources in IFW Dresden. Research Computing Center of Moscow State University²⁰ and The Center for Information Services and High Performance Computing of Technical University of Dresden are acknowledged for computing time. Financial support by DFG (projects PO 1602/1-2 to AAP and DU225/31-1 within the D-A-CH program) is highly appreciated

Notes and references

^a Leibniz Institute for Solid State and Materials Research, 01069 Dresden, Germany. E-mail: a.popov@ifw-dresden.de

[†] All structures were first optimized at the PBE/TZ2P level with core-effective potentials for Sc, La, and Br using Priroda code.²¹ Then, single point energy calculations at the PBE-D3 level with Grimme's dispersion correction with Becke-Johnson damping,²² DKH2 scalar relativistic correction and SARC-modification of def2-TZVP basis set²³ were performed using Orca suite.²⁴

Electronic Supplementary Information (ESI) available: CC bond lengths and POAV pyramidalization angles in $\text{LaSc}_2\text{N@C}_s(\text{hept})\text{-C}_{80}$, complete lists of cycloadducts with their relative energies, Cartesian coordinates. See DOI: 10.1039/c000000x/

1. A. A. Popov, S. Yang and L. Dunsch, *Chem. Rev.*, 2013, **113**, 5989; X. Lu, L. Feng, T. Akasaka and S. Nagase, *Chem. Soc. Rev.*, 2012, **41**, 7723; A. Rodriguez-Fortea, A. L. Balch and J. M. Poblet, *Chem. Soc. Rev.*, 2011, **40**, 3551; M. Rudolf, S. Wolfrum, D. M. Guldi, L. Feng, T. Tsuchiya, T. Akasaka and L. Echegoyen, *Chem.-Eur. J.*, 2012, **18**, 5136; M. N. Chaur, F. Melin, A. L. Ortiz and L. Echegoyen, *Angew. Chem.-Int. Edit.*, 2009, **48**, 7514.
2. S. Osuna, M. Swart and M. Solà, *Phys. Chem. Chem. Phys.*, 2011, **13**, 3585.
3. C. M. Cardona, *Curr. Org. Chem.*, 2012, **16**, 1095; X. Lu, L. Bao, T. Akasaka and S. Nagase, *Chem. Commun.*, 2014, **50**, 14701; X. Lu, T. Akasaka and S. Nagase, *Chem. Commun.*, 2011, **47**, 5942.
4. Y. Zhang, K. B. Ghiassi, Q. Deng, N. A. Samoylova, M. M. Olmstead, A. L. Balch and A. A. Popov, *Angew. Chem.-Int. Edit. Engl.*, 2015, **52**, 495.
5. M. Maggini, G. Scorrano and M. Prato, *J. Am. Chem. Soc.*, 1993, **115**, 9798.
6. C. M. Cardona, A. Kitaygorodskiy and L. Echegoyen, *J. Am. Chem. Soc.*, 2005, **127**, 10448; N. Chen, E. Y. Zhang, K. Tan, C. R. Wang and X. Lu, *Org. Lett.*, 2007, **9**, 2011.
7. S. Aroua and Y. Yamakoshi, *J. Am. Chem. Soc.*, 2012, **134**, 20242; T. Cai, Z. X. Ge, E. B. Iezzi, T. E. Glass, K. Harich, H. W. Gibson and H. C. Dorn, *Chem. Commun.*, 2005, 3594.
8. S. Aroua, M. Garcia-Borràs, S. Osuna and Y. Yamakoshi, *Chem.-Eur. J.*, 2014, **20**, 14032.
9. T. Cai, C. Slebodnick, L. Xu, K. Harich, T. E. Glass, C. Chancellor, J. C. Fettinger, M. M. Olmstead, A. L. Balch, H. W. Gibson and H. C. Dorn, *J. Am. Chem. Soc.*, 2006, **128**, 6486; A. Rodriguez-Fortea, J. M. Campanera, C. M. Cardona, L. Echegoyen and J. M. Poblet, *Angew. Chem.-Int. Edit.*, 2006, **45**, 8176; S. Aroua, M. Garcia-Borràs, M. F. Bölter, S. Osuna and Y. Yamakoshi, *J. Am. Chem. Soc.*, 2014, DOI: 10.1021/ja511008z.
10. R. C. Haddon and L. T. Scott, *Pure Appl. Chem.*, 1986, **58**, 137.
11. M. M. Olmstead, H. M. Lee, J. C. Duchamp, S. Stevenson, D. Marciu, H. C. Dorn and A. L. Balch, *Angew. Chem.-Int. Edit.*, 2003, **42**, 900.
12. S. Osuna, M. Swart and M. Sola, *J. Am. Chem. Soc.*, 2009, **131**, 129.
13. C. Bingel, *Chem. Ber.-Recl.*, 1993, **126**, 1957; A. Hirsch, I. Lamparth and H. R. Karfunkel, *Angew. Chem.-Int. Edit. Engl.*, 1994, **33**, 437.
14. A. Hirsch and M. Brettreich, *Fullerenes. Chemistry and Reactions.*, Wiley-VCH Verlag GmbH & Co. KGaA, Weinheim, 2005.
15. T. Cai, L. Xu, C. Shu, H. A. Champion, J. E. Reid, C. Anklin, M. R. Anderson, H. W. Gibson and H. C. Dorn, *J. Am. Chem. Soc.*, 2008, **130**, 2136.
16. O. Lukoyanova, C. M. Cardona, J. Rivera, L. Z. Lugo-Morales, C. J. Chancellor, M. M. Olmstead, A. Rodriguez-Fortea, J. M. Poblet, A. L. Balch and L. Echegoyen, *J. Am. Chem. Soc.*, 2007, **129**, 10423; J. R. Pinzon, T. M. Zuo and L. Echegoyen, *Chem.-Eur. J.*, 2010, **16**, 4864; N. Alegret, M. N. Chaur, E. Santos, A. Rodriguez-Fortea, L. Echegoyen and J. M. Poblet, *J. Org. Chem.*, 2010, **75**, 8299.
17. N. Alegret, A. Rodríguez-Fortea and J. M. Poblet, *Chem.-Eur. J.*, 2013, **19**, 5061.
18. T. Cai, L. Xu, C. Shu, J. E. Reid, H. W. Gibson and H. C. Dorn, *J. Phys. Chem. C*, 2008, **112**, 19203.
19. N. Alegret, P. Salvadó, A. Rodríguez-Fortea and J. M. Poblet, *J. Org. Chem.*, 2013, **78**, 9986.
20. V. V. Voevodin, S. A. Zhumatiy, S. I. Sobolev, A. S. Antonov, P. A. Bryzgalov, D. A. Nikitenko, K. S. Stefanov and V. V. Voevodin, in *Open Systems J.*, 2012, p. <http://www.osp.ru/os/2012/07/13017641>.
21. D. N. Laikov and Y. A. Ustynuk, *Russ. Chem. Bull.*, 2005, **54**, 820; D. N. Laikov, *Chem. Phys. Lett.*, 1997, **281**, 151.
22. S. Grimme, J. Antony, S. Ehrlich and H. Krieg, *J. Chem. Phys.*, 2010, **132**, 154104; S. Grimme, S. Ehrlich and L. Goerigk, *J. Comput. Chem.*, 2011, **32**, 1456.
23. D. A. Pantazis and F. Neese, *J. Chem. Theory Comput.*, 2009, **5**, 2229; D. A. Pantazis, X.-Y. Chen, C. R. Landis and F. Neese, *J. Chem. Theory Comput.*, 2008, **4**, 908.
24. F. Neese, *WIREs Comput. Mol. Sci.*, 2012, **2**, 73.